

Investigations on Sensitivity of Modal Fibre-Interferometer for Acoustic Detection

Alexandre C. T. Santos^{1,2}^a, Ricardo M. Ribeiro²^b, Andrés P. L. Barbero²^c,
Taiane A. M. G. de Freitas²^d and Cláudia B. Marcondes³^e

¹*Instituto de Pesquisas da Marinha (IPqM), Rio de Janeiro/RJ, Brazil*

²*Departamento de Engenharia de Telecomunicações, Universidade Federal Fluminense (UFF), Niterói/RJ, Brazil*

³*Centro Federal de Educação Tecnológica Celso Suckow da Fonseca (CEFET-RJ), Rio de Janeiro/RJ, Brazil*

Keywords: Acoustic Communications, Michelson Interferometer, Opto-Acoustic Receiver, Modal Interferometer, Ultrasound, Modalmetric.

Abstract: This paper describes investigations on sensitivity of modal fibre-interferometer named as “modalmetric”, which is inserted in two optical coupling circuits based on circulator and 2x2 fibre-coupler. The “modalmetric” in reflective structure is simply a single-mode fusion spliced with a short or long piece of a sensitive multi-mode fibre (s-MMF) with a cleaved or mirrored end. All the devices presented here were probed in the C-band and the tests were carried out at ~ 43 kHz frequency. By using a circulator, an increased opto-acoustic sensitivity could be reached by misalignment of a FC/PC connection in the single-mode fibre, thus suggesting the excitation of higher order modes in addition to the fundamental LP₀₁. By using a 2x2 fibre-coupler, an increased sensitivity was observed when one of the arms was made more reflective from the FC/PC ferrule termination, thus suggesting a combination of modalmetric with Michelson interferometer or alternatively a type of light recycling that oscillates between the reflective terminations. This paper also shows successful tests of acoustic transmission through a 9.5cm length metallic billet. The central motivation is future applications of the modalmetric-based devices on ultrasonic communication and monitoring through solid media.

1 INTRODUCTION

Telecommunication links and networks are almost always based on the use of electromagnetic carriers. In the optical domain, the use of fibres to convey the light carrier predominates despite the distances involved. In the radiofrequency domain, electromagnetic waves typically presenting frequencies from kHz to many GHz can carry information through the free air in many types of wireless services.

However, many physical media hinder or even prohibit electromagnetic propagation suitable for communications. Thus, ultrasonic communication is practically the unique possibility. Some examples regarding almost only acoustic communications can

be cited as: petroleum (Rudraraju, 2010), solid media (Heifetz et al, 2018) (Wang et al, 2018), energy cables (Trane et al, 2015), downhole (Ahmad et al, 2014), metallic pipes (Chakraborty et al, 2015) and undersea environment (Farr et al, 2010).

Piezoelectric transducers (PZTs) have been used as acoustic emitter (and also as detector) due to their compactness, sensitivity, and availability (Sun et al, 2013). Fibre-optic detectors, especially those based on fibre Bragg gratings (FBGs) and interferometers provide the advantageous characteristics of optical sensors as: immunity to electromagnetic interference (EMI), large bandwidth, electric isolation, and others. Interferometric sensors based on single-mode fibre (SMF) are more common than on multimode (MMF)

^a <https://orcid.org/0000-0001-9478-179X>

^b <https://orcid.org/0000-0002-3169-6675>

^c <https://orcid.org/0000-0002-9077-8283>

^d <https://orcid.org/0000-0003-0721-0089>

^e <https://orcid.org/0000-0001-8002-1968>

owing to sensitivity ~ 1000 times larger than the latter (Layton et al., 1979). Hydrophones based on SMF (Meng et al., 2021), are sophisticated devices and in general require a great fibre length span.

The modalmetric device that will be presented here, is of a very simple construction, and is proposed intending to be useful for digital communication and works by selecting/restr and constraints the interfering modes traversing the SM/MM splice. It is recognized that FBG (Wild and Hinckley, 2011) and interferometric sensors may present comparable or even higher sensitivity than PZT-based sensors (Moccia et al., 2012). It was reported the acoustic communications through a metallic wall using PZT transducer as a transmitter and an FBG as a receiver by means of differential detection using PSK modulation (Wild and Hinckley, 2011). Therefore, opto-acoustic detectors may present advantages when compared to a piezoelectric one.

Modalmetric interferometer sensors in the reflective structure (R-MMI) are fabricated by simply splicing single-mode fibre (SMF) with the sensitive multimode fibre (s-MMF) (Freitas et al., 2020). It does not require the use of a FBG itself neither the careful control of interrogation, i.e., the “spectral alignment” between the laser and the grating spectrum. The R-MMI structures behave like a one-arm interferometer. Such R-MMIs structures have been used as a distributed disturbance detector operating in the electrical frequency’s domain (Oanca et al., 1997) (Ribeiro and Balod, 2018).

This paper investigates the sensitivity of two versions of the optical circuit of an opto-acoustic detector based on a lumped R-MMI structure. The sensitivity under 42.9 kHz acoustic frequency is characterized when the ultrasonic wave amplitude excitation is varied. In a first version, using an optical circulator to light-coupling, the sensitivity increase is investigated after the properly adjustment of a FC/PC connection that is inline inserted with the SMF link. In a second version, investigations of sensitivity were performed by using a 2x2 fibre-coupler, where one of the arms should be made more reflective from the ferrule termination. Furthermore, the paper not only shows opto-acoustic detection in a back-to-back configuration, but as well a transmission along 9.5-cm length of a metallic billet.

2 EXPERIMENTAL

Figures 1a-1d sketch the four built experimental setups comprising the two optical circuit versions of the modalmetric detector: using circulator (Figs.1a

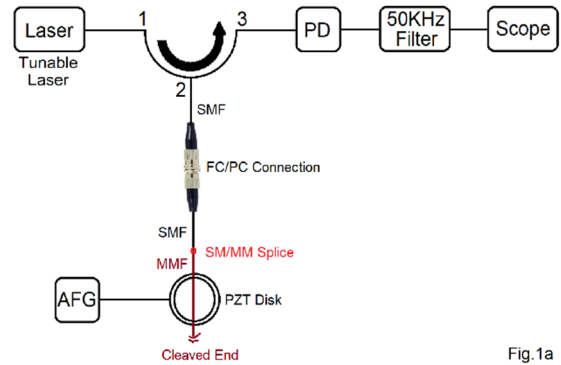


Fig.1a

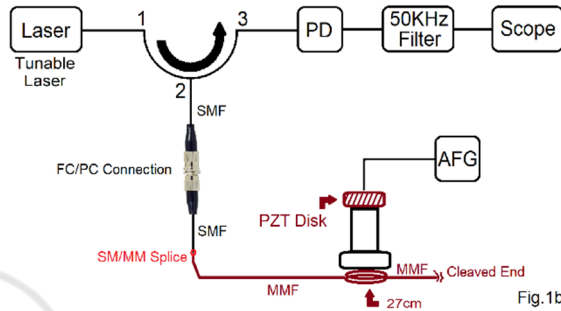


Fig.1b

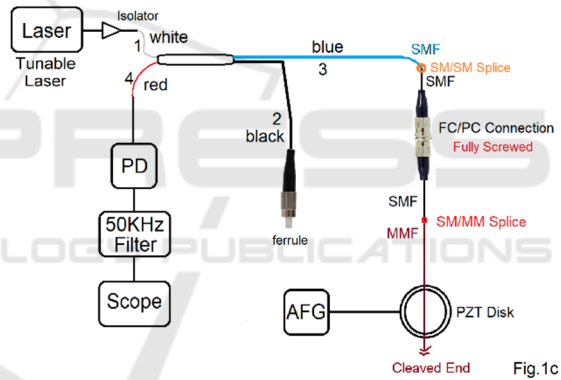


Fig.1c

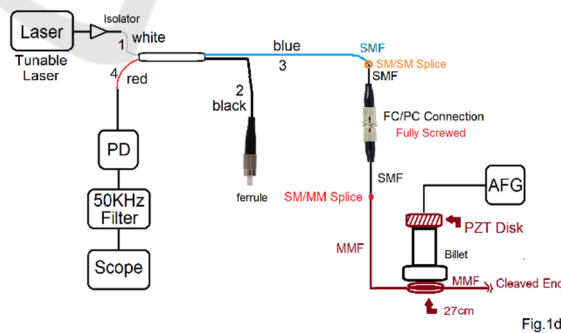


Fig.1d

Figures 1: Experimentals setups of the opto-acoustic modal-interferometric detector.

and 1b) and using an 2x2 fibre-coupler (Figs.1c and 1d). The probe light is launched into port 1 and exits at port 2 of an optical circulator or into port 1 and exits port 2 and 3 of an 2x2 fibre-optic coupler. Figure 1a shows a back-to-back transmission configuration

using a continuous probe from an external-cavity tunable laser (C-band) as light source. Figures 1b-1d show an acoustic transmission in back-to-back or through a 9.5-cm length of a metallic billet using a continuous 1550nm DFB laser as light source.

The used SI-SMF (9 μ m/125 μ m) and GI-MMF (62.5 μ m/125 μ m) were both of standard Telecom-grade. The probe optical signal propagates along the SMF until reach the sensitive MMF (s-MMF). The s-MMF is fusion spliced to the output port of the circulator or fibre-coupler. The SMF length from splice to the SMF/SMF-FC/PC connector was ~ 65 cm as shown in Fig. 1a. The higher-order $> LP_{01}$ modes excitation even in the SMF (Schulze et al, 2013), is achieved by properly adjusting the SMF/SMF-FC/PC connector as will be better explained in the next section. The free end of MMF was simply cleaved and none mirroring was applied. The light signal at < 1 mW optical power level, as reflected by the cleaved end of the s-MMF, modulated (or not) by the acoustic waves, is recovered by the optical circulator/2x2 fibre-coupler.

A SMD50T25F45R model PZT ultrasonic transducer disc from STEMiNC is used to generate acoustic waves. The disc was made with SM111 ceramic, presents 50 mm and 2.5 mm diameter and thickness, respectively. The (44 \pm 3) kHz was specified by the manufacturer as the radial mode resonance frequency. In communications and monitoring is generally expected the arrival of very weak acoustic signals. Therefore, there is no effort here to generate high power ultrasound. An arbitrary function generator (AFG) directly provides and excites the PZT disc with a 1-tone 42.9 kHz frequency electrical carrier that matches the effective resonance frequency of the disc. The AFG provided 0 – 12.5 Vpp voltage range. The PZT disc generates and transfers the acoustic waves directly to the s-MMF (Fig.1a and 1c) or through a metallic billet (Fig. 1b and 1d).

Figure 1a and 1c show 50 mm length (L_{MM}) of s-MMF strand that was glued over the face and along the diameter of the PZT disc by using a cyanoacrylate-based adhesive.

The reflected light by cleaved end of the s-MMF is collected by the port 3 of the circulator or port 4 of the 2x2 fibre-coupler and reaches the preamplified PIN photodetector (Thorlabs - PDA 10CS). In the setup of Fig. 1a, the PDA was pre-amplified at 30 dB (4.75 x 10⁴ Ω) and the remained setups (Figs. 1b-1d) the PDA was set at 40 dB (1.51 x 10⁵ Ω) transimpedance gain (TIA) level for high impedance input load corresponding to 775 kHz or 320 kHz bandwidth, respectively. The output of the

photodetector was connected to the $f_c = 50$ kHz electrical band-pass filter (EBPF). The filtered output signals were displayed and recorded by means of analog or digital oscilloscopes.

The SMF was fusion spliced to a 62.5/125 μ m s-MMF strand leading to reflective modalmetric device. As can be seen in Figs. 1b and 1d, ~27 cm length s-MMF was coiled in 5 turns with ~1.7 cm diameter which was laid and glued using a cyanoacrylate-based adhesive over the internal surface of a metallic box with ~ 2 mm thickness just in contact with the billet with 9.5 cm length and 6.4 cm diameter by means of bottom surface. Therefore, the s-MMF presents ~27 cm of physical interaction length with the vibrating surface. It should be pointed out that the device works in reflective mode and the effective interaction length is really the double of the ~27 cm s-MMF physical length. By using an acoustic couplant gel, the PZT disc was put in physical contact in the top surface of the billet.

3 RESULT AND DISCUSSIONS

3.1 Optical Circulator + Modalmetric Setup in Back-to-Back Acoustic Transmission

The laser was tuned to 1551.5 nm wavelength and $P_{in} = 5.7$ mW was the optical power fed to the s-MMF. Because the s-MMF end was simply cleaved, a maximum of 0.035 x 5.7 mW \approx 200 μ W (-7 dBm) optical power could be back reflected to the photodetector. The TIA gain was set to 30 dB.

Figure 2 shows two dependences of output voltage amplitude (mVpp) from the detector device of Fig. 1a when the excitation voltage amplitude (Vpp) applied on the PZT disc is varied in the ~ 0 - 10 V range. The vertical axis means the output voltage signal as captured by the oscilloscope. In the first dependence, the FC/PC connectors were “fully screwed” thus concentrically aligning both the SMF cores. The dependence is clearly sublinear. In the second dependence, it was kindly unscrewed one of the sides of the adapter that contains the SMF FC/PC connectors, keeping the other side totally close. The FC/PC connector were very slightly misaligned and carefully fitted to obtain a maximum output amplitude (“fitted max. sensitivity”) when 10Vpp voltage excitation is applied. Almost none transmitted optical power variation was observed in such procedure by using an optical power meter. However, it was observed that the amplitude of the signal

showed at the scope became greater, when compared with the “fully screwed” connectors. It is likely that by means of a slightly lateral with/without additional angular misalignment, higher-order modes than the fundamental LP_{01} are also excited in the fibre core (Ivanov et al, 2006) (Freitas et al, 2020) (Schulze et al, 2013). Since the distance along the SMF from the SM/MM splice to the FC/PC connector is over $<1\text{m}$, the high-order modes can survive and excites high-order modes in the s-MMF. By using this strategy, the sensitivity could be increased. In the reverse sense, it was reported the near-field contour of the light propagating along the SMF after the back coupling from the MMF (Ivanov et al, 2006). Most of the modulated content is propagating along the cladding and higher-order modes through the core. A similar behavior was reported where an amplitude enhancement of the signal was achieved after lateral misalignment from 0.9 to $6.8\ \mu\text{m}$ of the fibre’s core but in the SMF/MMF fusion splice out of the concentric fitting (Ribeiro and Balod, 2018). Similarly, the angular misalignment by using the SM-FC/APC with MM-PC connection can also enhances the modalmetric sensitivity (Visagathilagar et al, 2014) (Freitas et al, 2020). However, in this paper is shown that the mode excitation can be carried out even in the SMF link, i.e., by merely adjusting the FC/PC-FC/PC connection and monitoring (optimizing) the output signal amplitude.

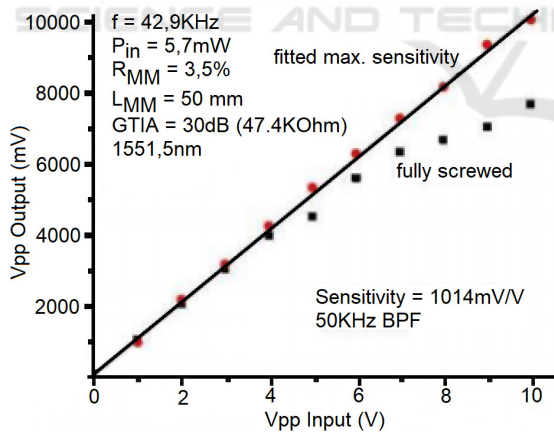


Figure 2: Sensitivity dependences of the modalmetric device using an optical circulator in B2B.

Figure 2 shows a linear dependence when the FC/PC connector is adjusted as “fitted max. sensitivity”. A sensitivity of $1014\ \text{mVpp/Vpp}$ was calculated by linear regression. For excitation voltage amplitudes $> 4\ \text{Vpp}$ the sensitivity measured for “fitted max. sensitivity” is higher than for the “fully screwed” connector. The $1014\ \text{mVpp/Vpp}$ sensitivity

was $1014/87 \approx 11.7$ times greater than the $87\ \text{mVpp/Vpp}$ measured for the FBG-based opto-acoustic detector (Leal et al, 2018). By using the modalmetric detector, very weak acoustic signals as those generated by applying $< 0.05\ \text{Vpp}$ amplitude on the PZT disc was transduced to the optical domain with good fidelity. The same experiment was carried out with the FBG-based detector and only excitations of $> 0.5\ \text{Vpp}$ amplitude could be properly detected (Leal et al, 2018). Roughly speaking, the modalmetric-based optical detector using circulator presented $\sim 10\ \text{dB}$ higher sensitivity than the FBG-based device.

Figure 3 shows the dependence of output voltage amplitude (mVpp) from the device when the wavelength of the probing laser is tuned in the $1525\text{-}1625\ \text{nm}$ wavelength range and the FC/PC connection is in the “fully screwed” status. The excitation voltage amplitude applied on the PZT disc was $10\ \text{Vpp}$ and $5.7\ \text{mW}$ was again launched to the s-MMF.

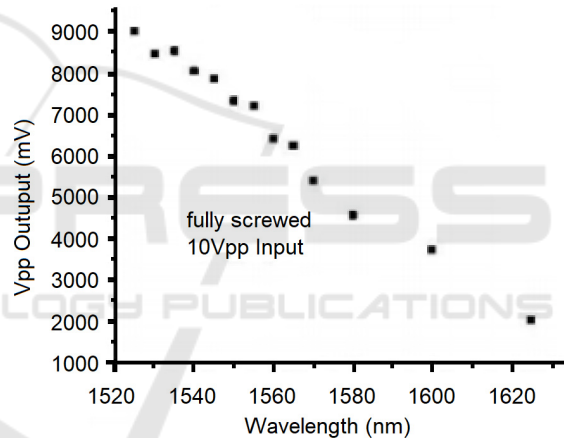


Figure 3: Sensitivity dependence of the modalmetric device using an optical circulator when the wavelength is made to vary in the $1525\text{-}1625\ \text{nm}$ range.

The graded-index MMF is ultimately an optical guide of multi-mode interference (MMI) type. The spectral response of such structure is periodic fringes where the periodicity decreases as the fibre length increases (Kumar et al, 2003). Because of the short length of the MMF used here, an incomplete oscillation occurs as shown in Fig. 3 where the maximum of transmission is close to $1525\ \text{nm}$.

Although the scope trace is not shown here, an improved sensitivity of $1340\ \text{mVpp/Vpp}$ was reached by properly fitting the SMF/SMF connection and probing the device with $1525\ \text{nm}$ wavelength. This leads a sensitivity of $1340/87 = 15.4$ times ($\sim 12\ \text{dB}$) the $87\ \text{mVpp/Vpp}$ reached by the FBG-based opto-acoustic detector (Leal et al, 2018).

3.2 Optical Circulator + Modalmetric Setup in Acoustic Transmission Through a Metallic Billet

Now, a DFB laser emitting around 1550 nm wavelength and $P_{in} < 5$ mW was the optical power launched to the s-MMF. The TIA gain was set to 40 dB. As is shown in the Fig. 1b, the acoustic waves propagate along the metallic billet thus resulting in a weak dynamic strain/stress that occurs due the arrival of ultrasound in the position where the glued modalmetric s-MMF is placed. The link was optimized by simple trial, i.e. by slightly changing the coupling position of the PZT-transmitters over the top surface of the billet.

Figure 4 shows the acoustic response, i.e. it shows the output voltage amplitude (Vpp) from the device detector when the excitation voltage amplitude (Vpp) applied on the PZT disc is varied in the $\sim 0 - 12.5$ V range. The FC/PC connector was “fully screwed”. The response is nonlinear thus presenting an approximate agreement with the B2B transmission shown by Fig. 2.

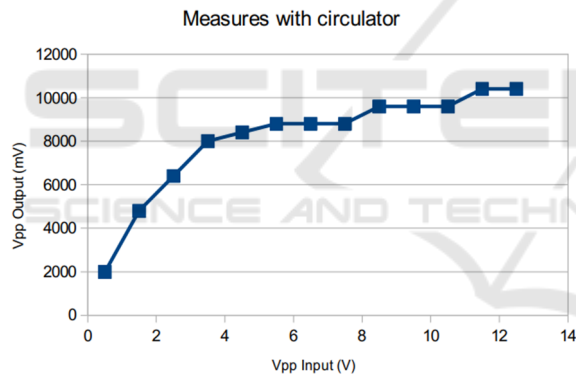


Figure 4: Sensitivity dependence of the modalmetric device using an optical circulator after propagation along 9.5 cm length of a metallic billet.

The average acoustic sensitivity from 0 to ~ 3 Vpp voltage amplitude excitation was extracted as to be ~ 2000 mV/V. This latter is greater than the 1014 mV/V obtained in B2B as shown in Fig. 2 because now the TIA gain is 40 dB instead of 30 dB. Therefore, the normalized sensitivity regarding the propagation along the billet is given by $2000/3.17 = 631$ mV/V. Furthermore, as was already reported (Freitas and Ribeiro, 2021), in B2B measurements using the same PZT-disc and 25 cm length of s-MMF, an average acoustic sensitivity of 1074 mV/V was achieved but constrained to the 0-1 V range of excitation. In the present paper, a normalized acoustic sensitivity of 631 mV/V with a good linearity at least in the 0 - 3V

amplitude range excitation is measured as seen from Fig. 4. An increase from 0 - 1V to 0 - 3V of the dynamic range is here observed due the acoustic attenuation after propagation along the billet thus reducing the ultrasound amplitude that strikes the s-MMF.

Although a similar result was previously published by our group (Ribeiro and Freitas, 2021), an important difference should nevertheless be noticed. In (Ribeiro and Freitas, 2021) and section 3.1, a tunable laser with 100 kHz linewidth, more powerful and of higher cost was used as a light source. In this sub-section, a DFB laser with ~ 10 MHz linewidth was used as the light source. So far, we have not carried out studies on the effect of the laser linewidth on the sensitivity of the modalmetric devices. However, from the results obtained, it seems that the performance difference is not significant at least for external-cavity and DFB lasers.

3.3 2x2 Fibre-Coupler + Modalmetric Setup in Back-to-Back Transmission

As is shown in the Fig. 1c, the optical circuit to couple the light is an 70/30 2x2 fibre-coupler where the acoustic waves are in back-to-back transmission. The FC/PC connector in the SMF was “fully screwed”. The optical probe of the s-MMF launched in the arm 3 was at 1.8 mW power level.

Figure 5 shows the acoustic sensitivity (mVpp) from the modalmetric detector when the excitation voltage amplitude (Vpp) applied on the PZT disc is varied in the $\sim 0 - 12.5$ V range. The acoustic sensitivity measurements were performed in three situations considering the arm 2 terminated by a FC/PC connector. In the first situation, the ferrule was immersed in a refractive index matching liquid so that the reflected signal was virtually null. The curve marked with blue squares shows a reduced sensitivity of $\sim 0.66/10 = 66$ mVpp/Vpp under 10 Vpp amplitude excitation. If we take into account that 1.8 mW is probing the s-MMF, $1.8 \times 0.035 = 63$ μ W power level is reflected by the cleaved end of s-MMF and < 63 μ W will reach the photo-detector. From the calibration plot of modalmetric response under the probing power level as can be seen from Fig. 4 of (Freitas *et al*, 2020), a sensitivity of $\ll 150$ mV/V is extrapolated and is in good agreement with the 66 mV/V measured even taking into account the 40 dB TIA amplifying gain. The circuit with 2x2 fibre-coupler, which presents free port (arm 2) terminated for null reflection, works only on the basis of the

modalmetric device as in the case of using the circulator, but with reduced sensitivity.

Hereafter, the ferrule of arm 2 was cleaned and dried so that it began to reflect $\sim 3.5\%$ of the light power. The curve marked with red diamond yields a sensitivity of $12/12.5 = 960 \text{ mVpp/Vpp}$ for 12.5 V voltage excitation amplitude. There was then a sensitivity increase of $960/66 = 14.5$ times when compared to the circuit working only as modalmetric. It should be noted that the behavior of the curve marked with red diamonds is not linear, which is consistent with the fact that we have here a “fully-screwed” FC/PC connector, similar to what was described in section 3.1. By extending the straight line between 0 and 4.5 Vpp of the curve marked with red diamonds, an extrapolated sensitivity of $\sim 20/12.5 = 1600 \text{ mVpp/Vpp}$ is obtained for 12.5 Vpp of voltage excitation amplitude.

Two possible interpretations are outlined here. The circuit using a 2×2 fibre-coupler with a free port (arm 2) terminated with $\sim 3.5\%$ reflection, works as one of the arms or reference arm of a fibre-optic Michelson interferometer. The other arm (arm 3) is the s-MMF, i.e. the reflective modalmetric device. When arm 2 is terminated with refractive index matching gel, the light arriving at the PD carries only the amplitude modulation generated from the splice when acoustic signals disturb the s-MMF. When the arm 2 (ferrule) is terminated with a free surface reflecting 3.5% of the light power, the visibility of the interferometer increases as the optical powers of arms 2 and 3 reaching the PD are more equalized. Thus, a possible interpretation for the higher sensitivity obtained with the Michelson configuration is that some *additional* phase modulation generated in the s-MMF that proceeds through the SMF will be converted into amplitude modulation when the optical signals from arm 2 and 3 overlap in the photodiode. Therefore, we will have two in-phase contributions to the output signal: 1st) Amplitude modulated signal due to the conversion of phase modulation acquired by modal interference (between modes) in the s-MMF which is converted into amplitude modulation from the SM/MM fusion splice. 2nd) Amplitude modulated signal generated from the Michelson interferometer itself that is formed by the SM fibers of the 2×2 fibre-coupler.

Another possible interpretation is that there may be an oscillation of light reflected and modulated on terminal 3 (cleaved end of the s-MMF) and also reflected on terminals 1 and 4. In this case, when terminal 2 starts to reflect some power of light, a higher level of such power starts to oscillate between arms 3 – (1 and 4), resulting in an increase in the

oscilloscope signal. This possibility is what is called “light recycling”, described for a Michelson interferometers in free-space aiming to detect gravitational waves (Sato et al, 2000).

In a third experiment, the FC/PC ferrule was placed in physical contact with a mirrored surface so that most of the light power level was reflected from arm 2. What was observed is that the signal disappeared for all launched acoustic signal values up to at least 12.5 Vpp . The circuit using a 2×2 fibre-coupler with a free port (arm 2) terminated with a mirror is causing virtually total reflection that saturates the TIA when set at 40 dB . However, when the TIA gain was reduced to 20 dB , an output signal could be observed with 2 Vpp amplitude for 10 Vpp excitation. Since the PDA saturates from 20 Vpp output, an extrapolation of $(3.17)^2 \times 2 \text{ Vpp} = 20 \text{ Vpp}$ output could be obtained by using 40 dB TIA gain. It can be inferred here that there must be an optimal reflection percentage to maximize the sensitivity of the device as a whole as illustrated in Fig. 1c.

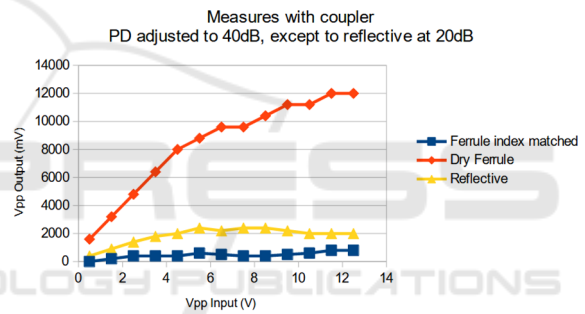


Figure 5: Sensitivity dependence of the modalmetric device using an 2×2 fibre-coupler in B2B transmission.

3.4 2×2 Fibre-Coupler + Modalmetric Setup in Acoustic Transmission Through a Metallic Billet

As is shown in the Fig. 1d, the optical circuit to couple the light is an 2×2 fibre-coupler 70/30 where the acoustic waves propagate along the 9.5 cm length billet thus in principle resulting in a very weak signal to be detected. The FC/PC connector in the SMF was “fully screwed”. The optical probe of the s-MMF launched in the arm 3 was done at 1.8 mW power level.

Figure 6 shows the acoustic sensitivity (mVpp) from the device detector when the excitation voltage amplitude (Vpp) applied on the PZT disc is varied in the $\sim 0 - 12.5 \text{ V}$ range. What can be seen from Fig. 6 is that they are essentially attenuated results when compared to the sensitivity plot of Fig. 5. For example, the dry ferrule produced sensitivities of

12/12.5 = 960 and $5.25/12.5 = 420$ mVpp/Vpp for 12.5 Vpp excitation voltage amplitude, respectively. The physical interpretations are the same as those given in section 3.3 for the B2B transmission configuration. We can compare the sensitivity of 420 mVpp/Vpp from Fig.6 referring to the 2x2 coupler, with 820 mVpp/Vpp from Fig. 4 referring to the circulator, both showing the sensitivity after transmission along the billet. The result shown in Fig. 6 refers to a 3.5% reflection from the ferrule of port 2. However, Fig. 6 shows that for 12.5 Vpp excitation voltage amplitude, an output of ~ 0.8 Vpp was achieved with high reflection from the terminal ferrule in arm 2, but with a TIA gain set to be only 10 dB. Normalizing this last result to that of Fig.5, we will have an extrapolated sensitivity of $(3.17)^3 \times 0.8 \sim 25.3$ Vpp, which gives, $25.3/12.5 \sim 2023$ mVpp/Vpp. Although it could be argued that the 0.8 Vpp signal contains some noise contamination, it should be noted that the 2x2 coupler offers more degrees of freedom to achieve increased sensitivity than when using the circulator.

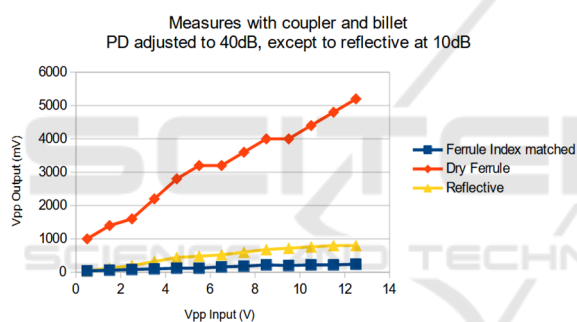


Figure 6: Sensitivity dependence of the modalmetric device using an 2x2 fibre-coupler in transmission through a 9.5 cm length billet.

4 CONCLUSIONS

This paper reported a modalmetric device which is of very simple construction, high sensitivity and can work as an opto-acoustic detector. The core of a modalmetric-based device is a short (or long) length of s-MMF fusion spliced or connectorized with a SMF. The optical circuit intended to couple, partially process and recover the light is here described to be a circulator or a 2x2 fibre-coupler. Below it is outlined some conclusions from the experimental results as described in the present paper:

1^a) By performing a lateral/angular misalignment in the FC/PC connector between SM fibres, it is possible to excite LP₀₁ as well higher-order modes (Schulze et al, 2013), thus resulting in a more

sensitive interferometric device. Of course, performing a misaligned fusion splice instead of connectorization is more practical and mechanically stable.

2^a) It is possible to increase the sensitivity of the modalmetric device by making it operate at a different wavelength, but closer to 1550 nm. In the present paper was 1525 nm, which is the lower limit of the tunable laser. The device sensitivities were measured as 1340 mVpp/Vpp that is ~ 12 dB greater than the sensitivities obtained with the FBG-based detector (Leal et al, 2018).

3^a) It appears that although the coherence (linewidth) of an external cavity laser or DFB differs by ~ 2 orders of magnitude, the sensitivity performance of the modalmetric is not significantly changed. An in-depth analysis of this point is left for a future research.

4^a) An improved transmission along a 9.5 cm length metallic billet with circulator and 2x2 coupler was demonstrated.

5^a) The circuit with 2x2 fibre-coupler presenting a free port (arm 2) terminated for null reflection, works only on the basis of the modalmetric device, as in the previous case of using the circulator.

6^a) The modalmetric circuit using a 2x2 fibre-coupler but with a free port (arm 2) terminated with $\sim 3.5\%$ reflectance presented a sensitivity higher than when is terminated with a null reflectance. In order to explain such behavior, two suggestions are here outlined: A superposition of modal and Michelson fibre interferences; and "light recycling" due oscillations inside the arms of Michelson interferometer (Sato et al, 2000). This is an interesting point to be explored in the future in order to combine multimodal interference with interference within single-mode fibre-optic circuits.

7^a) The circuit using a 2x2 fibre-coupler with a free port (arm 2) terminated with a mirror, causes virtually total reflection, thus yielding an extrapolated large sensitivity of 2023 mVpp/Vpp since the TIA gain is set at 10 dB in transmission through a billet. It can be inferred here that there may exist an optimal reflection percentage to maximize the sensitivity. This is left as a research suggestion for future works.

REFERENCES

- Ahmad, T. J., Noui-Mefidi, M. and Arsalan, M. (2014). Performance analysis of downhole acoustic communication in multiphase flow. *In 40th Annual Conference of the IEEE Industrial Electronic Society (IECON 2014)*. Dallas, TX.

- Chakraborty, S. *et al.* (2015). Low-power, low-rate ultrasonic communications system transmitting axially along a cylindrical pipe using transverse waves. In *IEEE Transaction Ultrasonic Ferroelectric Frequency Control*, Vol. 62, pp. 1788–1796.
- Farr, N., Bowen, A., Ware, J., Pontbriand, C. and Tivey, M. (2010). An integrated, underwater optical/acoustic communications system. In *IEEE Communications Magazine*.
- Freitas, T. A. M. G. and Ribeiro, R. M. (2021). The effects of scaling and bends in a fiber-optic modalmetric acoustic detector. In *Microwave and Optical Technology Letters*, Vol. 63, 2, pp. 708–713.
- Freitas, T. A. M. G., Silva, V. H. and Ribeiro, R. M. (2020). Sensitivity of fiber-based modalmetric devices intended for optical detection of acoustic signals. In *Microwave and Optical Technology Letters*, 62, 3, pp. 999–1008.
- Heifetz, A., Vilim, R. B. and Bakhtiari, S. (2018). Transmission of information by acoustic communication along metal pathways in nuclear facilities. In *Argonne National Laboratory, Report ANL-18/35*.
- Ivanov, O. V., Nikitov, S. A. and Gulyavev, Y. V. (2006). Cladding modes of optical fibers: properties and applications. In *Physics-Uspekhi*, 49 (2), pp. 167–191.
- Kumar, A., Varshney, R. K., Antony, S. C. and Sharma, P. (2003). Transmission characteristics of SMS fiber optic sensor structures. In *Optics Communications* 219, 215–221.
- Leal, W. A., Carneiro, M. B. R., Freitas, T. A. M. G., Marcondes, C. B. and Ribeiro, R. M. (2018). Low-frequency detection of acoustic signals using fiber as an ultrasonic guide with a distant in-fiber Bragg grating. In *Microwave and Optical Technology Letters*, 60, 4, pp. 813–817.
- Moccia, M., Consales, M., Iadicicco, A., Pisco, M., Cutolo, A., Gladi, V. and Cusano, A. (2012). Resonant hydrophones based on coated fiber Bragg gratings. In *Journal of Lightwave Technology*, 30, 15, 2472–2481.
- Oanca, I., Yang, G.Y., Katsifolis, J and Tapanes, E. (1997). Simultaneous wavelength multiplexed fiber optic communications and cable integrity monitoring technique. In *CLEO, paper WP4*, 106.
- Ribeiro, R. M. and Balod, Y. C. (2018). Modalmetric interferometer under Fingerprint disturbances: The effect of lateral offset between the single-mode and multimode fiber splice. In *Microwave and Optical Technology Letters*, 60, 1, pp. 151–157.
- Ribeiro, R. M. and Freitas, T. A. M. G. (2021). Modalmetric Detector in an Acoustic Transmission Along Metallic Medium. In *2021 SBMO/IEEE MTT-S International Microwave and Optoelectronics Conference (IMOC), Fortaleza, Brazil, 24-27 October*.
- Rudraraju, R. (2010). Ultrasonic data communication through petroleum. In *Master of Science Thesis, University of Akron*.
- Sato, S. *et al.* (2000). High-gain power recycling of a Fabry-Perot Michelson interferometer for a gravitational-wave antenna. In *Applied Optics*, 39, 25, pp. 4616–4620.
- Sun, Z., Rocha, B., Wu, K.-T. and Mrad, N. (2013) A Methodological Review of Piezoelectric Based Acoustic Wave Generation and Detection Techniques for Structural Health Monitoring. In *International J. of Aerospace Engineering*, v. 2013, article ID 928627, 22 pages.
- Schulze, C. *et al.* (2013). Measurement of higher-order mode propagation losses in effectively single mode fibers. In *Optics Letters*, 38, 23, pp. 4958–4961.
- Trane, G., Mijarez, R., Guevara, R. and Baltazar, A. (2015). PZT guided waves sensor permanently attached on multi-wire AWG12 cables used as communication medium. In *41st Annual Review of Progress in Quantitative Nondestructive Evaluation, AIP Conference Proceedings*. Boise, ID. (Vol. 1650, no. 1, pp. 631–639).
- Visagathilagar, Y., Katsifolis, J. and Koziol, B. (2014). Modalmetric fibre sensor. US Patent 8,792,754 B2, July 29, 2014.
- Wang, B., Saniie, J., Bakhtiari, S. and Heifetz, A. (2018). Software defined ultra-sonic system for communication through solid structures. In *2018 IEEE International Conference on Electro/Information Technology (EIT)*, Rochester, MI.
- Wild, G. and Hinckley, S. (2011). A fibre Bragg grating sensor as a receiver for acoustic communication signals. In *Sensors*, 11, 455–471.
- Layton, M. R. and Bucaro, J.A. (1979). Optical fiber acoustic sensor utilizing mode-mode interference. *Applied Optics*, vol 18, No. 5.
- Zhou MENG, Wei CHEN, Jianfei WANG, Xiaoyang HU, Mo CHEN, and Yichi ZHANG (2021). Recent Progress in Fiber-Optic Hydrophones. In *Photonic Sensors*, 2021, 11(1): 109–122.